Journal of Sound and Vibration (2001) **245**(2), 363–374
doi:10.1006/jsvi.2000.3515, available online at http://www.idealibrary.com on IDEAL®

VIBRATIONS OF A NON-IDEAL PARAMETRICALLY AND SELF-EXCITED MODEL

J. WARMINSKI

Department of Applied Mechanics, Technical University of Lublin, Nadbystrzycka 36 *street,* 20-618 *Lublin, Poland. E-mail*: *jwar@archimedes.pol.lublin.pl*

J. M. BALTHAZAR

Department of Applied Mathematics, State University of São Paulo at Rio Claro, PO Box 178, 13500-230 *Rio Claro, SP, Brazil. E-mail*: *jmbaltha@rc.unesp.br*

AND

R. M. L. R. F. BRASIL

Department of Structural and Foundations Engineering, Polytechnic School, University of São Paulo, PO Box 6151, 05424-930 *SP, Brazil. E-mail*: *rmldrbr@usp.br*

(*Received* 27 *July* 2000, *and in final form* 12 *October* 2000)

1. ON NON-IDEAL SYSTEMS

When a forcing function F is independent of the system it acts on, then the forcing function is called ideal. Formally, the excitation may be expressed as a pure function of time. For example consider a system driven by a sinusoidal excitation $F = A\cos(\omega_{dr}t)$ having frequency ω_{dr} and amplitude A. In this case, the excitation is completely independent of the system response: that is, regardless of the motion the excitation imparts on the system the system never manifests any influence on the excitation source. In contrast, a forcing function dependent on the response of the system is said to be non-ideal.

If in a certain model its ideal source is replaced by a non-ideal source the excitation can be put in the form $F(\Phi)$, where Φ is a function which depends on the response of the system. Therefore, a non-ideal source cannot be expressed as a pure function of time, but rather as an equation that relates the source to the system of equations that describes the system. Hence, non-ideal systems always have one additional degree of freedom as compared with similar ideal systems.

Consider a motor operating on a structure. A certain input (power) is required to produce a certain output (RPM) regardless of the motion of the structure. For non-ideal systems this may not be the case. Hence, it is interesting to analyze what happens to the motor (input, output), as the response of the system changes. Here, the excitation is always limited in two senses: by the characteristic curves of the particular energy source (the motor, in this case) and by dependence of the motion of the system on the motion of the energy source. Coupling between the governing equations of the motion and the energy source then takes place.

The greatest interaction between the vibrating system and the energy source occurs at resonance, that is,

$$\frac{\mathrm{d}\phi}{\mathrm{d}t} - p = O(\varepsilon),$$

0022-460X/01/320363 + 12 $35.00/0

where $d\phi/dt$ is the angular velocity of the rotor (energy source), p is the natural frequency of the system, and ε is a small parameter of the problem.

As a consequence, in the regions of resonance, unstable conditions of motion may occur, the form of the vibrations is changed, and the character of the transition of the system through resonance is altered. The problem of passage through resonance of vibrating systems has drawn special attention of engineering researchers in recent years.

In non-ideal vibrating systems, it is well known that sometimes the passage through resonance requires more input power than is available. As a consequence the vibrating system cannot pass through resonance or requires an intensive interaction between the vibrating system and the energy source to be able to do it. The worst case is that in which the vibrating system will become stuck in resonance, just before resonance conditions are reached. Strong interaction leads to fluctuating motor speed and fairly large vibration amplitudes (the Sommerfeld effect of getting stuck in resonance). The motor may not have enough power to reach higher regimes with low energy consumption as most of its energy is applied to move the structure and not to accelerate the shaft.

In a classical book by Kononenko [1] the first detailed study on the non-ideal vibrating problem on the passage through resonance was presented. After this publication, the problem of passing through resonance has been investigated by a number of authors and some essential results were found, as discussed in references [2–5], for example.

If the region before resonance is considered in a typical frequency response curve, one notes that as the power supplied to the source increases, the RPM of the motor increases accordingly. However, this behaviour does not continue indefinitely. The closer the motor speed moves toward the resonance frequency, the more power the source requires to increase the motor speed. In other words, a large change in the power supplied to the motor results in a small change in the frequency and in a large increase in the amplitude of the resulting vibrations. Thus, near resonance it appears that additional power supplied to the motor will only increase the amplitude of the response with little effect on the RPM of the motor.

Finally, jump phenomena and the increase in power required by a source operating near resonance are some of the manifestations of a non-ideal energy source. In fact, the vibrating response provides a certain energy sink. One of the problems faced by designers is how to drive a system through resonance and avoid this kind of energy sink.

2. A MODEL OF PARAMETRICALLY AND SELF-EXCITED SYSTEM

A remarkable feature of systems exhibiting limit cycles is that the amplitude of the stationary motion does not depend on the initial conditions of vibrating system but on the system parameters. Stable limit cycles generally enclose a singular point representing a position of unstable equilibrium, so that vibrations build up and sustain themselves in the absence of external forces. For this reason such vibrations are called self-excited vibrations [6]. Self-excited vibrations have been examined by many authors in the current literature, as an example, a non-ideal (stick-slip) self-excited vibrating system has been investigated in reference [7] and the ideal model in reference [8].

Interaction between parametric and self-excited system has been presented in reference [9], where vibrations of an ideal van der Pol–Mathieu oscillator have been examined. A special effect, which is called a synchronization phenomenon, was observed in that system. Parametric vibrations pull in self-excited vibrations near parametric resonance regions. Outside these regions the system vibrates quasi-periodically with modulation amplitude. A non-ideal system with self, parametric and external excitation was investigated in detail in reference [10]. A dry friction model of self-excitation and linear parametric excitation was considered in this paper. Two stable solutions with similar amplitudes in a resonance area were obtained for that model, for ideal as well as for non-ideal source of energy.

Recently, an ideal self-excited system vibration with parametric and external excitations was investigated in references [11, 12] for Rayleigh–Mathieu oscillator. An additional small external excitation forcing the parametric and self-excited system can cause significant qualitative and quantitative changes. When the external excitation is not high, there are additional solutions in the synchronization area. The amplitude frequency characteristic has an additional loop. There are five steady solutions in the main parametric resonance region, but only two are stable.

In references [11, 12] the authors considered an ideal, self-excited, parametric mechanical system with one degree of freedom, non-linear Duffing elasticity and non-linear parametric excitation, given by the non-dimensional differential equation

$$\ddot{X} + (-\alpha + \beta \dot{X}^2)\dot{X} + (1 - \mu \cos 2\phi)(1 + \gamma X^2)X = q \cos \phi. \tag{1}$$

The coefficients in the above equation are positive, small values. One can notice that equation (1) includes linear and non-linear parametric excitation terms.

Figure 1 shows a non-ideal model for this kind of problem, which is the goal of investigation of this paper.

The presence of the unbalanced mass m_0 in the non-ideal model (see Figure 1) alters the potential and kinetic energies of the ideal problem, considered in references [11, 12], in ΔV and ΔT, respectively. Then the expression of the Lagrangian function is expressed by

$$\Delta L = \Delta T - \Delta V \tag{2}$$

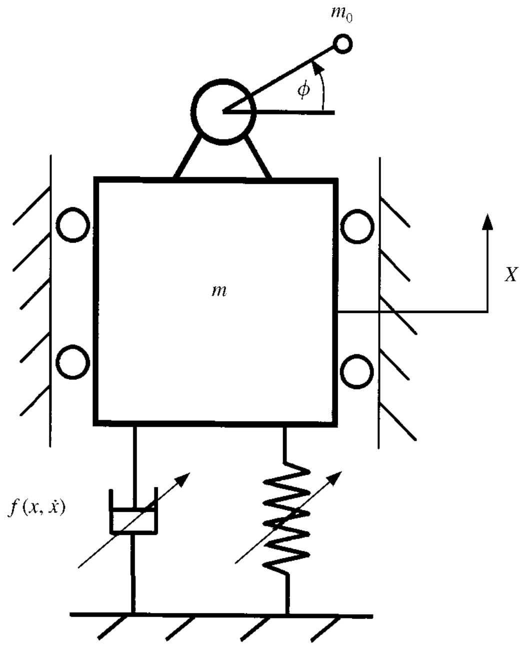

Figure 1. Non-ideal model of a parametrically and self-excited system.

where

$$\Delta V = m_0 g v_0, \qquad \Delta T = \tfrac{1}{2}\{m_0(\dot{v}_0^2 + \dot{u}_0^2) + I_0\dot{\phi}^2\}, \tag{3, 4}$$

with $v_0 = x + r\sin\phi$, $u_0 = r\cos\phi$.

In this way the non-ideal differential equations are written in the dimensionless form

$$\ddot{X} + (-a + \beta\dot{X}^2)\dot{X} + (1 - \mu\cos 2\phi)(1 + \gamma X^2)X = q(\ddot{\phi}\cos\phi - \phi^2\sin\varphi)$$

$$\ddot{\phi} = \eta(\ddot{x}\cos\phi - \dot{x}\phi\sin\phi) + \Gamma(\dot{\phi}), \qquad \dot{\phi} = \omega \tag{5}$$

where

$$\eta = \frac{m_0 r}{m_0 r^2 + I_0}, \qquad \Gamma = \frac{T(\dot{\phi})}{m_0 r^2 + I_0} \tag{6, 7}$$

Characteristic curves of the energy source (DC motor) are assumed to be straight lines:

$$\Gamma = u_1 - u_2\dot{\phi}. \tag{8}$$

Note that the parameter u_1 is related to the voltage and u_2 is a constant for each model of motor considered. The voltage is the parameter control of the problem.

The main purpose of this paper is to discuss the non-ideal parametric and self-excited vibrations of the system defined by Figure 1, whose equations are those given in equations (5).

An asymptotic solution of equation (5) and the stability analysis of the solution is presented in sections 3 and 4. In section 4 numerical simulations are carried out and finally in section 5 some concluding remarks are given.

3. ASYMPTOTIC ANALYSIS

In this paper some hypotheses for the non-ideal vibrating system defined by equations (5) are adopted. It is assumed that the system vibrates near the main parametric resonance, where the excitation frequency ϑ is close to the natural frequency p ($p = 1$), while the parametric excitation frequency is 2ϑ.

Introducing a small parameter ε, one can write:

$$p - \omega = \varepsilon\Delta. \tag{9}$$

One can also assume that the motion of the system takes place around the steady state. This means that the second derivative $\ddot{\phi}$ is not large. Upon expressing parameters of equations (5) by

$$\alpha = \varepsilon\tilde{\alpha},\ \beta = \varepsilon\tilde{\beta},\ \gamma = \varepsilon\tilde{\gamma},\ \mu = \varepsilon\tilde{\mu},\ q = \varepsilon\tilde{q},\ \eta = \varepsilon\tilde{\eta},\ \Gamma(\dot{\phi}) = \varepsilon\tilde{\Gamma}(\dot{\phi}),$$

the differential equations of motion take the form

$$\ddot{X} + p^2 X = \varepsilon\{(\tilde{\alpha} - \tilde{\beta}\dot{X}^2)\dot{X} + \tilde{\mu}X\cos 2\phi - \tilde{\gamma}X^3 + \tilde{\mu}\tilde{\gamma}X^3\cos 2\phi + \tilde{q}\ddot{\phi}\cos\phi - \phi^2\sin\phi\},$$

$$\ddot{\phi} = \varepsilon\{\tilde{\Gamma}(\dot{\phi}) + \tilde{\eta}\ddot{X}\cos\phi\}. \tag{10}$$

Next, by following reference [1], equations (10) are transformed into new co-ordinates A, ϕ, ψ, where

$$X = A\cos(\phi + \psi),\ \dot{X} = -\,Ap\sin(\phi + \psi),\ \dot{\phi} = \omega \tag{11}$$

and the second derivative of X has the form

$$\ddot{X} = -\frac{dA}{dt}p\sin(\phi+\psi) - \left(\omega + \frac{d\psi}{dt}\right)Ap\cos(\phi+\psi). \tag{12}$$

Taking into account equations (11) and (12) one obtains

$$\frac{dA}{dt}\cos(\phi+\psi) - \frac{d\psi}{dt}A\sin(\phi+\psi) = (\omega - p)\;A\sin(\phi+\psi). \tag{13}$$

Substituting equations (11), (12) and (13) into the differential equations of motion (10) yields

$$\begin{aligned}\frac{dA}{dt}p\sin(\phi+\psi) &+ \frac{d\psi}{dt}Ap\cos(\phi+\psi) - Ap(p-\omega)\cos(\phi+\psi) = \varepsilon\Big\{Ap(\tilde{\alpha} + \tfrac{3}{4}\tilde{\beta}p^2A^2)\sin(\phi+\psi)\\ &+ \tfrac{1}{4}A^3p^3\tilde{\beta}\sin 3(\phi+\psi) - \tfrac{1}{2}A\tilde{\mu}\cos(\phi-\psi) - \tfrac{1}{2}A\tilde{\mu}\cos(3\phi+\psi) + \tfrac{3}{4}A^3\tilde{\gamma}\cos(\phi+\psi)\\ &+ \tfrac{1}{4}A^3\gamma\cos 3(\phi+\psi) - \tfrac{3}{8}A^3\tilde{\gamma}\tilde{\mu}\cos(\phi-\psi) - \tfrac{3}{8}A^3\tilde{\gamma}\tilde{\mu}\cos(3\phi+\psi) - \tfrac{1}{8}A^3\tilde{\gamma}\tilde{\mu}\cos(\phi+3\psi)\\ &- \tfrac{1}{8}A^3\tilde{\gamma}\tilde{\mu}\cos(5\phi+3\psi) + \tilde{q}\omega^2\sin\phi - \tilde{q}\,\frac{d\omega}{dt}\cos\phi\Big\},\end{aligned} \tag{14}$$

$$\frac{d\omega}{dt} = \varepsilon\left\{\tilde{\Gamma}(\omega) - \tilde{\eta}p\left[\frac{dA}{dt}\sin(\phi+\psi) + A\left(\omega + \frac{d\psi}{dt}\right)\cos(\phi+\psi)\right]\cos\phi\right\}.$$

Equations (13) and (14) lead to the derivatives $d\omega/dt$, dA/dt, $d\psi/dt$:

$$\frac{d\omega}{dt} = \varepsilon\{\tilde{\Gamma}(\omega) - Ap\tilde{\eta}\omega\cos\phi\cos(\phi+\psi)\},$$

$$\begin{aligned}\frac{dA}{dt} = \varepsilon\Big\{&\frac{\tilde{q}\omega^2}{p}\sin\phi + A\tilde{\alpha}\sin(\phi+\psi) - \frac{3}{4}A^3p^2\tilde{\beta}\sin(\phi+\psi) + \frac{1}{4}A^3p^2\tilde{\beta}\sin 3(\phi+\psi)\\ &- \frac{A\tilde{\mu}}{2p}\cos(\phi-\psi) - \frac{A\tilde{\mu}}{2p}\cos(3\phi+\psi) + \frac{3}{4}\frac{A^3\tilde{\gamma}}{p}\cos(\phi+\psi) + \frac{1}{4}\frac{A^3\tilde{\gamma}}{p}\cos 3(\phi+\psi)\\ &- \frac{3}{8}\frac{A^3\tilde{\gamma}\tilde{\mu}}{p}\cos(\phi-\psi) - \frac{3}{8}\frac{A^3\tilde{\gamma}\tilde{\mu}}{p}\cos(3\phi+\psi) - \frac{1}{8}\frac{A^3\tilde{\gamma}\tilde{\mu}}{p}\cos(\phi+3\psi)\\ &- \frac{1}{8}\frac{A^3\tilde{\gamma}\tilde{\mu}}{p}\cos(5\phi+3\psi)\Big\}\sin(\phi+\psi) + \varepsilon^2, \ldots\end{aligned}$$

$$\frac{d\psi}{dt} = \varepsilon\left\{\Delta + \frac{\tilde{q}\omega^2}{Ap}\sin\phi + \tilde{\alpha}\sin(\phi+\psi) - \frac{3}{4}A^3p^2\tilde{\beta}\sin(\phi+\psi) + \frac{1}{4}A^2p^2\tilde{\beta}\sin 3(\phi+\psi)\right.$$

$$+\frac{3}{4}\frac{A^2\tilde{\gamma}}{p}\cos(\phi+\psi) + \frac{1}{4}\frac{A^2\tilde{\gamma}}{p}\cos 3(\phi+\psi) - \frac{1}{2}\frac{\tilde{\mu}}{p}\cos(\phi-\psi) - \frac{1}{2}\frac{\tilde{\mu}}{p}\cos(3\phi+\psi)$$

$$-\frac{3}{8}\frac{A^2\tilde{\gamma}\tilde{\mu}}{p}\cos(\phi-\psi) - \frac{3}{8}\frac{A^2\tilde{\gamma}\tilde{\mu}}{p}\cos(\phi-\psi) - \frac{3}{8}\frac{A^2\tilde{\gamma}\tilde{\mu}}{p}\cos(3\phi+\psi)$$

$$\left.-\frac{1}{8}\frac{A^2\tilde{\gamma}\tilde{\mu}}{p}\cos(\phi+3\psi) - \frac{1}{8}\frac{A^2\tilde{\gamma}\tilde{\mu}}{p}\cos(5\phi+3\psi)\right\}\cos(\phi+\psi) + \varepsilon^2, \ldots . \tag{15}$$

To solve equations (15) the classical method of Krylov–Bogoliubov–Mitropolski is applied [13]. According to this method, in the first approximation one can write

$$\omega = \Omega + \varepsilon U_1(\phi, \Omega, a, \xi), \quad A = a + \varepsilon U_2(\phi, \Omega, a, \xi), \quad \psi = \xi + \varepsilon U_3(\phi, \Omega, a, \xi), \tag{16}$$

where $U_1(\phi, \Omega, a, \xi)$, $U_2(\phi, \Omega, a, \xi)$, $U_3(\phi, \Omega, a, \xi)$ are slowly changing periodic functions of time. To find solutions for Ω, a, ξ in the first approximation, the right-hand sides of equations (15) are averaged,

$$\frac{d\Omega}{dt} = \frac{\varepsilon}{2\pi}\int_0^{2\pi} f_\Omega\, d\varphi, \quad \frac{da}{dt} = \frac{\varepsilon}{2\pi}\int_0^{2\pi} f_a\, d\varphi, \quad \frac{d\xi}{dt} = \frac{\varepsilon}{2\pi}\int_0^{2\pi} f_\xi\, d\varphi, \tag{17}$$

and after integration one obtains

$$\frac{d\Omega}{dt} = \varepsilon\left\{\Gamma(\Omega) - \frac{1}{2}ap\tilde{\eta}\Omega\cos\xi\right\},$$

$$\frac{da}{dt} = \varepsilon\left\{\frac{1}{2}\tilde{\alpha}a - \frac{3}{8}a^3p^2\tilde{\beta} - \frac{1}{4}a\frac{\tilde{\mu}}{p}\sin 2\xi - \frac{1}{8}a^3\frac{\tilde{\gamma}\tilde{\mu}}{p}\sin 2\xi + \frac{1}{2}\tilde{q}\frac{\Omega^2}{p}\cos\xi\right\},$$

$$\frac{d\xi}{dt} = \varepsilon\left\{\Delta + \frac{3}{8}a^2\frac{\tilde{\gamma}}{p} - \frac{1}{4}\frac{\tilde{\mu}}{p}\cos 2\xi - \frac{1}{4}\frac{\tilde{\gamma}\tilde{\mu}}{p}\cos 2\xi - \frac{1}{2}\tilde{q}\frac{\Omega^2}{ap}\sin\xi\right\}, \tag{18}$$

$$\frac{d\phi}{dt} = \Omega.$$

For the steady state, equations (18) have the form

$$\Gamma(\Omega) - \tfrac{1}{2}ap\tilde{\eta}\Omega\cos\xi = 0,$$

$$\frac{1}{2}\tilde{\alpha}a - \frac{3}{8}a^3p^2\tilde{\beta} - \frac{1}{4}a\frac{\tilde{\mu}}{p}\sin 2\xi - \frac{1}{8}a^3\frac{\tilde{\gamma}\tilde{\mu}}{p}\sin 2\xi + \frac{1}{2}\tilde{q}\frac{\Omega^2}{p}\cos\xi = 0,$$

$$\Delta + \frac{3}{8}a^2\frac{\tilde{\gamma}}{p} - \frac{1}{4}\frac{\tilde{\mu}}{p}\cos 2\xi - \frac{1}{4}\frac{\tilde{\gamma}\tilde{\mu}}{p}\cos 2\xi - \frac{1}{2}\tilde{q}\frac{\Omega^2}{ap}\sin\xi = 0. \tag{19}$$

Rectangular velocity, amplitude and phase of the vibrating system for a steady state are obtained from the solutions of equations (19).

4. ON THE STABILITY ANALYSIS

The analysis of the stability of periodic solutions is performed by using the approximate differential equations of the first order (18) which can be written in a shortened form:

$$\frac{\mathrm{d}\Omega}{\mathrm{d}t} = F_1(a, \Omega, \xi), \quad \frac{\mathrm{d}a}{\mathrm{d}t} = F_2(a, \Omega, \xi), \quad \frac{\mathrm{d}\xi}{\mathrm{d}t} = F_3(a, \Omega, \xi). \tag{20}$$

In steady state, equation (20) is equal to zero:

$$F_1(a, \Omega, \xi) = 0, \; F_2(a, \Omega, \xi) = 0, \; F_3(a, \Omega, \xi) = 0.$$

Upon taking into account the differences between perturbed and non-perturbed equations, the variational differential equations are written as follows:

$$\begin{aligned}
\frac{\mathrm{d}\delta_\Omega}{\mathrm{d}t} &= \left(\frac{\partial F_1}{\partial \Omega}\right)_0 \delta_\Omega + \left(\frac{\partial F_1}{\partial a}\right)_0 \delta_a + \left(\frac{\partial F_1}{\partial \xi}\right)_0 \delta_\xi, \\
\frac{\mathrm{d}\delta_a}{\mathrm{d}t} &= \left(\frac{\partial F_2}{\partial \Omega}\right)_0 \delta_\Omega + \left(\frac{\partial F_2}{\partial a}\right)_0 \delta_a + \left(\frac{\partial F_2}{\partial \xi}\right)_0 \delta_\xi, \\
\frac{\mathrm{d}\delta_\xi}{\mathrm{d}t} &= \left(\frac{\partial F_3}{\partial \Omega}\right)_0 \delta_\Omega + \left(\frac{\partial F_3}{\partial a}\right)_0 \delta_a + \left(\frac{\partial F_3}{\partial \xi}\right)_0 \delta_\xi.
\end{aligned} \tag{21}$$

The characteristic determinant of equations (21) has the form

$$\begin{vmatrix}
\left(\frac{\partial F_1}{\partial \Omega}\right)_0 \delta_\Omega - \rho & \left(\frac{\partial F_1}{\partial a}\right)_0 \delta_a & \left(\frac{\partial F_1}{\partial \xi}\right) \delta_\xi \\
\left(\frac{\partial F_2}{\partial \Omega}\right)_0 \delta_\Omega & \left(\frac{\partial F_2}{\partial a}\right)_0 \delta_a - \rho & \left(\frac{\partial F_2}{\partial \xi}\right) \delta_\xi \\
\left(\frac{\partial F_3}{\partial \Omega}\right)_0 \delta_\Omega & \left(\frac{\partial F_3}{\partial a}\right)_0 \delta_a & \left(\frac{\partial F_3}{\partial \xi}\right) \delta_\xi - \rho
\end{vmatrix} = 0. \tag{22}$$

The index '0' denotes partial derivatives of the F functions at the equilibrium point. The stability of the approximate solution (19) depends on the roots of the characteristic equation (22). Solutions are stable when eigenvalues of the characteristic equation have negative real parts. The numerical values of the eigenvalues will be presented in the next section.

5. ON NUMERICAL SIMULATION RESULTS

Numerical results were carried out by using a Matlab-Simulink® package. Calculations were done for different sets of the system parameters taken from the most interesting intervals of physical systems. Results of calculations were obtained for the following parameters [11, 12, 14],

$$\alpha = 0{\cdot}1, \; \beta = 0{\cdot}05, \; \gamma = 0{\cdot}1, \; \mu = 0{\cdot}2, \; q = 0{\cdot}2, \; \eta = 0{\cdot}3$$

and the characteristic of energy source was assumed as a straight line (see equation (8)),

$$\Gamma(\dot{\phi}) = u_1 - u_2\dot{\phi}$$

where u_1 is a control parameter and depends on voltage, and the u_2 parameter depends on the type of energy source. In the calculations, the control parameter is assumed as $u_1 \in (0{\cdot}6, 4{\cdot}0)$, and $u_2 = 1{\cdot}5$.

With account taken of the approximate equations (19) and by finding numerically the roots of the characteristic equation (22), the amplitude and a rectangular velocity were found and are plotted against the control parameter in Figure 2. Analytical results are denoted by AR, stable and unstable solutions are denoted by solid and dashed lines, respectively, and RKG are Runge–Kutta–Gill method results with a variable step length. The results shown in Figure 2 are analyzed according to three distinct regions: A, $\{u_1 \in (0{\cdot}6, 1{\cdot}3)\}$; B, $\{u_1 \in < 1{\cdot}3, 2{\cdot}5)\}$; C, $\{u_1 \in < 2{\cdot}5, 4)\}$.

The time history of the vibrational behaviour of the displacement and angular velocity in region A is shown in Figure 3(a). In this region one may observe quasi-periodic motion which is obtained by mutual interaction between self-excitation, parametric excitation and energy source (DC motor). This type of motion is marked in Figure 2 by two dots, denoting extreme deflections of the system. In region B, a kind of synchronization effect is observed. It has predomination of parametric and external excitation. An additional interesting effect in the synchronization region is visible. There are two maximas, resulting from a strong interaction between the vibrating system and energy source (limited power supply). Before going out from the synchronization area to region C (near $u_1 \approx 2{\cdot}4$) the system may vibrate periodically and quasi-periodically, depending on the chosen initial conditions. Finally, in region C the system vibrates quasi-periodically once more (see Figure 3(d)).

Similar effects connected with angular velocity are shown in Figure 2(b). It is also important to mention that if one slowly increases the voltage, inside the synchronization region, that is $u_1 \in (1{\cdot}2.\ 2{\cdot}4)$, one observes a decreasing of the angular velocity Ω. Time histories of the displacement X and angular velocity ω obtained from numerical simulations for characteristic u_1 parameters are presented in Figure 3. Quasi-periodic vibrations out of the synchronization region are presented in Figure 3(a) for $u_1 = 1{\cdot}3$, Figure 3(c) for $u_1 = 2{\cdot}4$

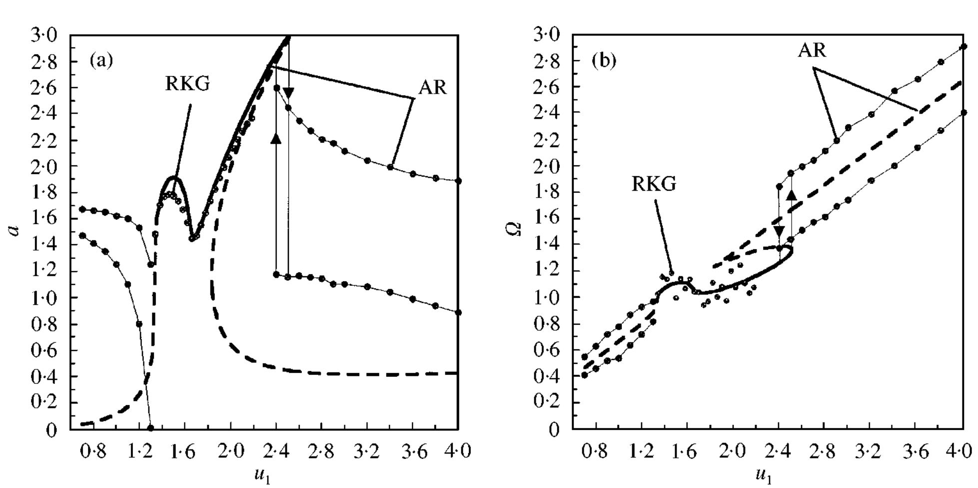

Figure 2. Amplitude (a) and angular velocity (b) versus control parameter u_1 near the main parametric resonance. AR, analytical results; RKG, numerical simulation.

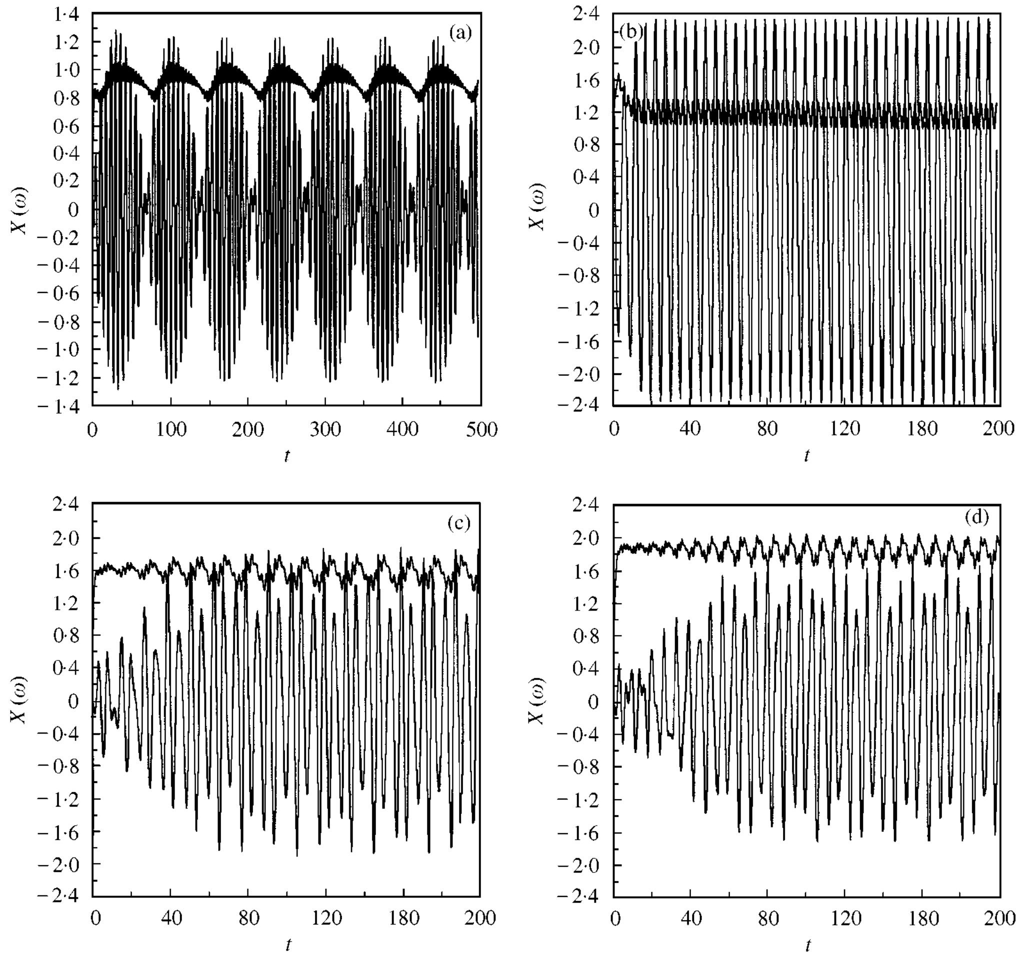

Figure 3. Displacement X and angular velocity ω; time histories for chosen control parameter u_1. (a) $u_1 = 1{\cdot}30$; (b) $u_1 = 2{\cdot}20$; (c) $u_1 = 2{\cdot}40$; (d) $u_1 = 2{\cdot}80$.

and Figure 3(d) for $u_1 = 2{\cdot}8$ respectively. For $u_1 = 2{\cdot}2$ the system is synchronized and vibrates periodically (see Figure 3(b)).

The amplitude versus angular velocity near the main parametric resonance obtained from asymptotic analysis (section 3) is presented in Figure 4. This resonance curve has an untypical shape. A zoom of this region shows peculiar behaviour. Inside the synchronization region an internal loop appears. It is possible to explain this by observing region B in Figure 2. Comparing amplitude and angular velocity characteristics in Figures 2(a, b) reveals local maxima for both curves. This affects directly the shape of the amplitude versus angular velocity curve in Figure 4. It is necessary to mention that this kind of internal loop appeared in the ideal model [11, 12]. Nevertheless, ideal and non-ideal loops have different meanings. For the ideal model the internal loop appears on the right branch of the resonance curve and only its upper part is stable. For the non-ideal system this kind of loop appears on the left branch and there are only stable solutions. This effect is caused by interaction between self- and parametric excitations and is due to the influence of the non-ideal source of energy.

It is possible to verify agreement between asymptotic and numerical results. In Figures 5 and 6 the passage through resonance with a slowly increasing and decreasing value of the

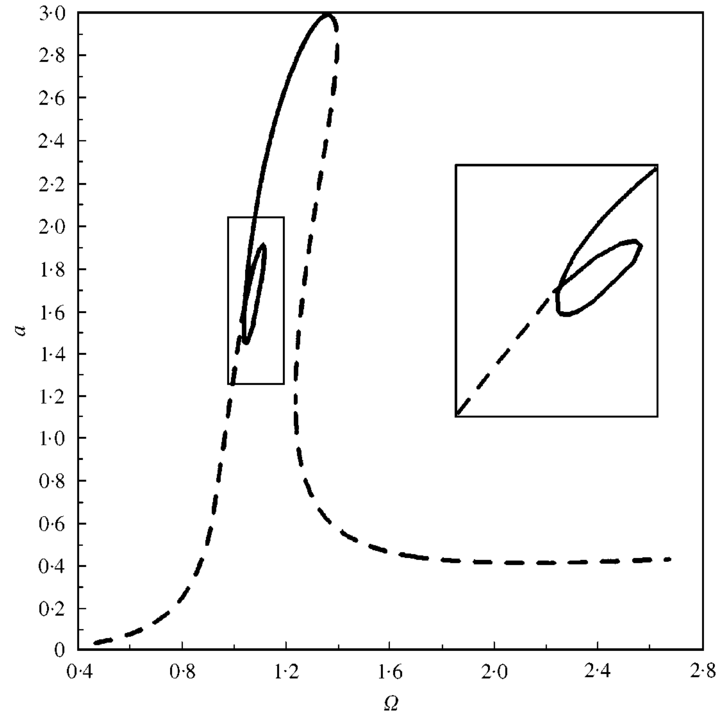

Figure 4. Amplitude versus angular velocity near the main parametric resonance.

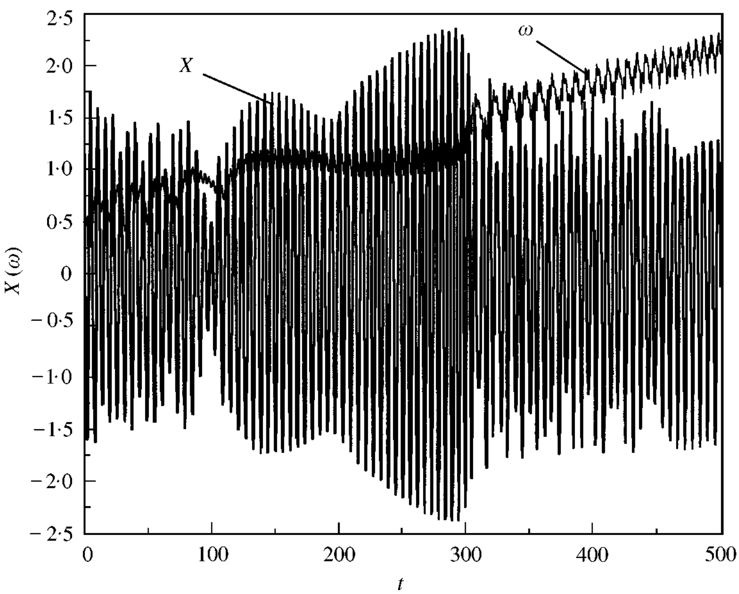

Figure 5. Transition through resonance with a slowly increasing value of control parameter u_1.

control parameter u_1 is presented. In these figures one can note that inside the resonance region, $t \in (100, 300)$ for increasing, and $t \in (240, 380)$ for decreasing, values of the control parameter u_1, two maximas of amplitude are visible. These results are in complete agreement with previous results shown in Figures 2 and 4.

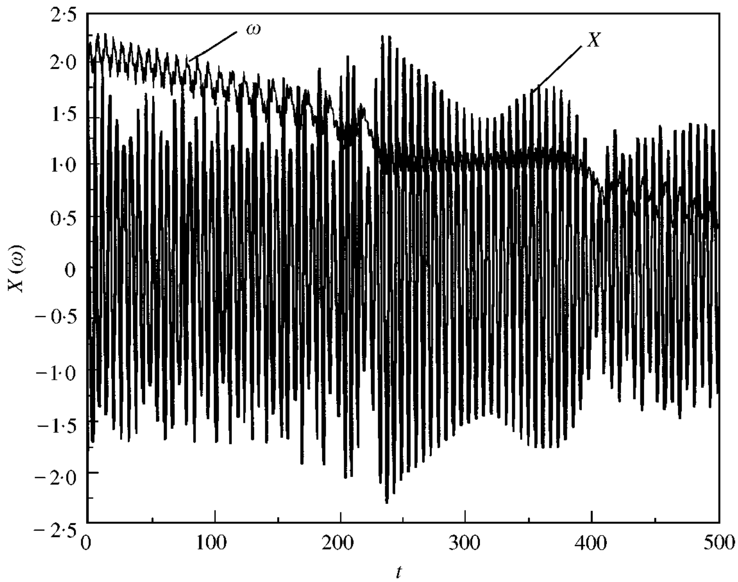

Figure 6. Transition through resonance with a slowly decreasing of control parameter u_1.

6. SOME CONCLUDING REMARKS

A non-ideal parametrically and self-excited vibrating model was investigated by analytical and numerical methods. Interaction between parametric and external excitation leads to the synchronization phenomenon. In the ideal model a kind of internal loop has been obtained in the synchronization region near the main parametric resonance. Nevertheless, only the upper part of the loop is stable and it appeared on the right branch of the resonance curve [11, 12]. New results for a non-ideal system have been obtained. Contribution of the non-ideal energy source is manifested by an internal stable loop inside the main parametric resonance. The loop is located on the left branch of the amplitude versus the angular velocity curve (see Figure 4). In this particular case the loop appears on a distinct part of the resonance diagram. This phenomenon is produced by interaction between self- and parametric excitation and the external non-ideal source of energy.

ACKNOWLEDGMENTS

This research was supported by the Polish Committee of Sciences grant No. 1001/T07/99/16 (J. Warminski). The second (J. M. Balthazar) and third author (R.M.L.R.F. Brasil) thank Conselho Nacional de Pesquisas (CNPq), a Brazilian funding agency, for financial support.

REFERENCES

1. V. O. Kononenko 1969 *Vibrating Systems with Limited Power Supply*. London: Illife.
2. J. M. Balthazar, B. I. Cheshankov, D. T. Ruschev, L. Barbanti and H. I. Weber 2001 *Journal of Sound and Vibration* **239**, 1075–1085. Remarks on the passage through resonance of a vibrating system with two degrees of freedom.

3. H. Yamakawa and S. Nurakami 1989 in *Current Topics in Structural Mechanics* (H. Chung editor) PVP-Vol. 179, 181–185. New York: American Society of Mechanical Engineers. Optimum designs of operating curves for rotating shaft systems with a limited power supply.
4. S. Suherman 1996 *Ph.D. Dissertation, Virginia Polytechnic Institute and State University*. Transient analysis and vibrating suppression of a cracked rotating shaft with a ideal and non-ideal motor passing through a critical speed.
5. R. M. Dimentberg, L. McGovern, R. L. Norton, J. Chapdelaine and R. Harrisson 1997 *Journal of Nonlinear Dynamics* **13**, 171–187. Dynamics of an unbalanced shaft interacting with a limited power supply.
6. L. Meirovitch 1971 *Methods of Analytical Dynamics*. New York: McGraw-Hill.
7. B. R. Pontes, V. A. Oliveira and J. M. Balthazar 2000 *Journal of Sound and Vibration* **234**, 713–723. On friction-driven vibrations in a mass block-belt-motor driven with a limited power supply.
8. B. R. Pontes, V. A. Oliveira and J. M. Balthazar 2000 in *2nd International Conference on Control of Oscillations and Chaos, Saint-Petersburg, Russia*, 5–7 July (F. I. Chernousko and A. L. Fradkov, editors), 171–172. A note on Melnikov's chaos criterion: results for a friction-drive self-excited vibrating systems.
9. A. Tondl 1978 *Monographs and Memoranda* **25**, *National Research Institute for Machine Design, Prague*. On the interaction between self-excited and parametric vibrations.
10. A. A. Alifov and K. W. Frolov 1985 *Interaction of Nonlinear Oscillatory Systems with Energy Sources* (in Russian). Moscow: Nauka.
11. K. Szabelski and J. Warminski 1995 *Journal of Non-Linear Mechanics* **30**, 179–189. The parametric self excited non-linear system vibrations analysis with the inertial excitation.
12. K. Szabelski and J. Warminski 1995 *Journal of Sound and Vibration* **187**, 595–607. Self-excited system vibration with parametric and external excitations.
13. N. N. Bogoliubov and J. A. Mitropolsky 1958 *Asymptotic Methods in Non-linear Vibrations Theory*. Moscow: GIF-ML.
14. J. M. Balthazar, M. L. Rente, V. M. David, D. T. Mook and H. I. Mook 1997 in *Nonlinear Dynamics, Chaos, Control and Their Applications to Engineering Sciences* (J. M. Balthazar, D. T. Mook and J. M. Rosario, editors), 97–104. Some observations on numerical simulations of a non-ideal dynamical system.